Joint Occurrence of Heatwaves and Ozone Pollution and Increased Health Risks in Beijing, China: Roles of Synoptic Weather Pattern and Urbanization

Lian Zong[1]，Yuanjian Yang[1,*], Haiyun Xia[1,*], Meng Gao[2], Zhaobin Sun[3], Zuofang Zheng[3], Xianxiang Li[4], Guicai Ning[5], Yubin Li[1], Simone Lolli[6]

[1]Collaborative Innovation Centre on Forecast and Evaluation of Meteorological Disasters, Key Laboratory for Aerosol-Cloud-Precipitation of China Meteorological Administration, School of Atmospheric Physics, Nanjing University of Information Science & Technology, Nanjing, China.
[2]Department of Geography, Hong Kong Baptist University, Hong Kong, China.
[3]Institute of Urban Meteorology, China Meteorological Administration, Beijing, China.
[4]School of Atmospheric Sciences, Sun Yat-Sen University, Guangzhou, China.
[5]Department of Land Surveying and Geo-Informatics, The Hong Kong Polytechnic University, Hong Kong, China.
[6]CNR-IMAA, Contrada S. Loja, 85050 Tito Scalo (PZ), Italy

Correspondence to: Prof. Yuanjian Yang (yyj1985@nuist.edu.cn) and Prof. Haiyun Xia (hsia@ustc.edu.cn)

Abstract. Heatwaves (HWs) paired with higher ozone (O_3) concentration at surface level pose a serious threat to human health. Their combined modulation of synoptic patterns and urbanization remains unclear. By using five years of summertime temperature and O_3 concentrations observation in Beijing, this study explored potential drivers of compound HWs and O_3 pollution events. Three unfavourable synoptic weather patterns were identified to dominate the compound HWs and O_3 pollution events. The weather patterns contributing to enhance those conditions are characterized by sinking air motion, low boundary layer height, and hot temperatures. Under the synergistic stress of HWs and O_3 pollution, the public mortality risk increased by approximately 12.59% (95% confidence interval: 4.66%, 21.42%). Relative to rural areas, urbanization caused higher risks for HWs, but lower risks for O_3 over urban areas. In general, unfavourable synoptic patterns and urbanization can enhance the compound risk of events in Beijing by 45.46% and 8.08%, respectively. Our findings provide robust evidence and implications for forecasting compound heatwaves and O_3 pollution event and its health risks in Beijing or in other urban areas all over the word having high concentrations of O_3 and high-density populations.

Key words: Heatwaves, ozone pollution, compound health risks, synoptic weather pattern, urbanization

1 Introduction

Climate warming and rapid urbanization have led to an increase in the frequency and duration of extreme high-temperature episodes (Lehner et al., 2018; Meehl & Tebaldi, 2004; Wang et al., 2021b; Yang et al., 2017; Li, 2020), to the point that they are recognized as one of the most serious types of meteorological disaster worldwide. Prolonged extreme high-temperature exposure can induce an increase in the morbidity and mortality due to cardiovascular and respiratory diseases, posing a serious

Atmospheric
Chemistry
and Physics
Discussions

threat to human health (Patz et al., 2005; Xu et al., 2016). Together with the rapid development of economic globalization and urbanization, human activities and the changes in the urban underlying surface have enhanced urban hyperthermia and frequent air pollution issues (Chew, et al., 2021; Li et al., 2016; Luo & Lau, 2018, 2019; Meehl et al., 2007; Rastogi, 2020; Wang et al.,

35   2007; Yang et al., 2020; Zheng et al., 2020). Heat waves (HWs) paired with the urban heat island (UHI) effect exposes urban residents to more sustained extreme high temperatures (Chew et al., 2021; Jiang et al., 2019; Tan et al., 2010; Wang et al., 2017; Zong et al., 2021b). The strong solar radiation and high temperatures in summer have accelerated the photochemical reaction, which is a proxy to the production and accumulation of O_3 (Herring et al., 2019; Shu et al., 2016; Zanis et al., 2000, 2011). In particular, O_3 became the main pollutant in summer (Fan et al., 2020; Gao et al., 2020b; Li et al., 2019; Wang et al.,

40   2019; Saikawa et al., 2017), and thus residents may suffer from dual health risks brought about by high temperatures and O_3 exposure in summer.

Accumulating epidemiological evidence shows that the coefficient of the O_3 concentration–response relationship for mortality in summer is higher (Atkinson et al., 2012; Pattenden et al., 2010; Pope et al., 2016; Zhong et al., 2019), suggesting that the health effects and mortality related to O_3 pollution are exacerbated by hot temperatures. Therefore, the significant increase in

45   O_3 concentrations during summertime is also greatly responsible for the increase in excess mortality; high temperatures and O_3 have a joint impact on public health (Hertig et al., 2020; Katsouyanni et al., 1993; Lelieveld et al., 2014; Pattenden et al., 2010). Numerous studies have been devoted to the individual impacts of a single extreme high-temperature or air pollution event on human health (Ma et al., 2015; Ning et al., 2020; Wang et al., 2020; Wong et al., 2013; Xu et al., 2016). However, with the co-occurrence of extreme HW and O_3 pollution events in summer becoming more frequent, it is imperative to reveal

50   the underlying mechanisms of extreme HW–O_3 compound events and improve the level of risk assessment related to extreme events in urban areas (Sartor et al. 1995; Hertig et al., 2020).

Beijing, the capital of China, is the second largest city in the country, with a permanent population of 21.89 million, making it one of the fastest developing metropolises in recent decades. Rapid urbanization and urban expansion have induced changes in land-use types, which in turn have changed the energy budget within the city boundary layer (Dou et al., 2015; Li et al.,

55   2015; Wang et al., 2007; Yu et al., 2013; Zheng et al., 2018; Zinzi et al., 2020). Urban areas usually experience warmer temperatures compared with rural areas (Oke and Maxwell, 1975; Rizwan et al., 2008; Roth, 2007; Stewart and Oke, 2012), and this strong UHI effect can be observed in Beijing all year around (Ren et al., 2007; Wang et al., 2017; Yang et al., 2013). As a result, urban residents are more vulnerable to health risks posed by heat stress. On the other hand, the increased O_3 concentration induced by urbanization was found to translate to a 39.6% increase in premature mortality (Yim et al., 2019).

60   Importantly, whilst urban greening might alleviate the UHI effect (Doick et al., 2014; Zhou et al., 2019), the additional biogenic volatile organic compounds (VOCs) emitted from vegetation under high-temperature stress can favour O_3 production (Ma et al., 2019; Wang et al., 2021a; Werner et al., 2020). For example, Ma et al. (2019) found that the landscape in Beijing yields an extra 4.47 ppbv of MDA8 O_3 (the maximum daily 8-h average concentration of O_3) due to the increase in urban isoprene emissions associated with HWs, and the isoprene emitted from forests in rural areas should also not be underestimated. But

65   what roles do synoptic weather patterns and urbanization play in the formation of complex HW–O_3 compound events in Beijing

with its high population density? What are the public health effects caused by these compound events? These important scientific issues warrant further investigation.

Therefore, the present study on extreme HW–O_3 compound events that occurred in Beijing during summertime of 2014–2019 was carried out to comprehensively investigate the roles of synoptic weather patterns and urbanization in these joint events

70 based on surface observation and reanalysis data. Then, the contributions of weather types and urbanization to the excess mortality brought about by combined heat and O_3 stress were quantified according to the established health assessment model of Liu et al. (2021) and Yin et al. (2017). The findings are expected to provide a scientific reference for the monitoring and forecasting of summertime HW–O_3 compound events and their health risks in Beijing from the perspective of synoptic patterns and urbanization.

75 **2 Data and Methods**

2.1 Data

Ground-level O_3 observation data during summertime (June–August) of 2014–2019 were retrieved from Beijing Municipal Ecological and Environmental Monitoring Center, ultimately comprising 31 air quality stations (11 for urban stations, 11 for rural stations, three for traffic stations, and six for other stations) with a missing-values rate for the O_3 concentration of less

80 than 10%.

In order to better assess the relationship between O_3 pollution and the meteorological variables, we selected 29 automatic weather stations (AWSs) closest to the environmental monitoring stations from the high-density AWS network (Figure 1; Table 1). Hourly 2-m air temperature, relative humidity (RH), the daily maximum temperature (T_{max}), and 10-m wind speed (WS) were obtained from the National Meteorological Information Center of the China Meteorological Administration, and

85 then heat index (HI) was retrieved as shown in Rothfusz (1990) as Eq. (1):

$$HI = -42.379 + 2.04901523 \times T + 10.14333127 \times RH - 0.22475541 \times T \times RH - 0.00683783 \times T^2 - 0.05481717 \times RH^2 + 0.00122874 \times T^2 \times RH + 0.00085282 \times T \times RH^2 - 0.00000199 \times T^2 \times RH^2, \qquad (1)$$

Where T indicates the temperature (unit: °F), and RH (unit: %) indicates relative humidity.

In addition, we also used the hourly geopotential height (GH), boundary layer height (BLH), wind vector, vertical velocity and

90 temperature fields to further analyze the weather type and local boundary layer characteristics under the joint occurrence of HW and O_3 pollution (Fifth major global reanalysis produced by the European Centre for Medium-Range Weather Forecasts, with spatiotemporal resolution of 0.25°).

2.2 Methods

2.2.1 Compound HW and O₃ pollution events

95 An HW event is usually characterized by the daily maximum temperature reaching or exceeding a certain threshold (it can be a relative value or an absolute threshold) for several consecutive days (Ngarambe et al., 2020). In this paper, we selected 33°C (which corresponds to the 90th percentile of T_{max} during 2014–2019 in Beijing) as threshold for T_{max} lasting for 3 days or more to determine an HW event; otherwise, it was a non-heat wave (NHW) event. Moreover, the occurrence of precipitation during the day inhibits the photochemical reaction of O₃ production (Yu et al., 2020; Zhang et al., 2015; Zhao and Wang, 2017), here

100 a daytime precipitation event (accumulated precipitation ≥ 2 mm during 0700–1900 LST) was excluded to avoid the impact of precipitation on compound HW and O₃ pollution events. O₃ pollution was identified as when the MDA8 O₃ concentration exceeded 160 μg m$^{−3}$, which is in accordance with the Ambient Air Quality Standards issued by the Ministry of Ecology and Environment of the People's Republic of China. Based on the above criteria, 84 days of co-occurring HW and O₃ pollution events during 2014–2019 were finally obtained.

2.2.2 Weather type classification

105 According to previous studies (Han et al., 2020; Miao et al., 2019; Ning et al., 2019; Yang et al., 2018, 2021; Zhang and Villarini, 2019), T-mode principal component analysis (T-PCA) was applied to classify the 850-hPa GH field of the joint occurrence of HW and O₃ pollution events [more specific details on T-PCA were introduced in our previous study (Zong, et al., 2021a)]. As for the categorical data, we mainly focused on the domain (110°–125°E, 32°–47°N), including Beijing, associated with these 84 days of compound events during summertime (June–August) 2014–2019.

2.2.2 Excess mortality

In epidemiology, the relative risk (RR) is usually used to evaluate the intensity of the association between exposure and disease, which refers to the ratio of the incidence of the exposed group to the incidence of the non-exposed group (Chen et al., 2018; Pope et al., 2016). The RR is calculated by Eq. (2):

115 $$RR_i = exp^{\beta_i * \Delta X_i}, \tag{2}$$

where i indicates the risk factor (high temperature or O₃ concentration), β_i is the exposure response function between the risk factor i and total mortality through nonlinear regression (Cao et al., 2021; Du et al., 2020; Gu et al., 2018), ΔX_i is the difference between the risk factor i and its reference health threshold. The excess risk (ER) is calculated by Eq. (3):

$$ER_i = (RR_i - 1) \times 100\%, \tag{3}$$

120 Here, we refer to the exposure response function for the high temperature as suggested by Liu et al. (2021), and O₃ concentration as suggested by Yin et al. (2017) in northern China. In detail, Liu et al. (2021) investigated the mortality caused by high temperature in 84 cities in China from 2013 to 2016, and found that for every 1°C increase in the daily T_{max} above 31.5°C, the largest RR of mortality caused by high temperature in northern China was 1.002 [95% confidence interval (CI):

Atmospheric
Chemistry
and Physics
Discussions

Open Access

125   1.001, 1.004]. For O$_3$ exposure, a 10-µg m^{-3} increase in MDA8 O$_3$ was related to an increase in the total daily mortality of 0.39% (95% CI: 0.04%, 0.75%) in northern China during the warm season (Yin et al., 2017). Since the two models have removed the mutual influence, the final joint ER is the sum of the ERs of both high temperature and O$_3$.

2.2.3 Urbanization and Synoptic contribution rates

To estimate the impact of urbanization and weather patterns on compound HW and O$_3$ pollution events, we further determined their contribution rates to the excess mortality of compound events. With reference to Ma & Yuan (2021), the urbanization

130   effect is calculated by Eq. (4):

$$\Delta ER_{i,urbanization} = ER_{i,urban} - ER_{i,rural}, \tag{4}$$

and contribution rate is calculated by Eq. (5):

$$CR_{i,urbanization} = \frac{\Delta ER_i}{ER_{i,urban}} \times 100\%, \tag{5}$$

Where i indicates risk factor (high temperature or ozone pollution), ER is excess mortality, and CR is contribution rate.

135   Similarly, we also defined synoptic effects as Eq. (6):

$$\Delta ER_{i,synoptic} = ER_{i,synoptic} - ER_{i,average}, \tag{6}$$

and the contribution rate as Eq. (7):

$$CR_{i,synoptic} = \frac{\Delta ER_i}{ER_{i,synoptic}} \times 100\%, \tag{7}$$

Where i, ER, and CR are same as Eq. (6).

140   **3 Results**

3.1 Compound HW–O$_3$ pollution events and associated public health in Beijing

Figure 2 shows the time series of the HW days, NHW days, O$_3$ pollution, and precipitation days, showing that HW periods (approximately 79.2% of HW days, Figure 3b) in Beijing, were always paired above-threshold O$_3$ pollution levels. Daytime precipitation obviously inhibits the photochemical reaction with consequent fewer O$_3$ pollution episodes occurred during

145   daytime precipitation (the average 24-h O$_3$ concentration was reduced by 17.14 µg m^{-3} on precipitation days compared with NHW days). Note that there was an increase in the maximum duration of HW events and the number of HW–O$_3$ paired days during summertime of 2014–2019 (Figure 3, by 2019, the most durable HW event lasted for 10 days), resulting in people suffering from more enduring dual heat and O$_3$ stress. As shown in Figure 4, MDA8 O$_3$ aggravated significantly on HW days, exceeding 160 µg m^{-3} across all stations, with an average of 189.35 µg m^{-3}. Nevertheless, also during NHW days, some MDA8

150   O$_3$ stations (mainly urban or vegetation covered stations) exceeded the pollution threshold. Both surface O$_3$ concentration and MDA8 O$_3$ concentration in Beijing showed significant differences ($P < 0.01$) among three conditions (Table 2). We further investigated the diurnal variation for surface air temperature (T), RH, HI, BLH and WS under HW, NHW and precipitation

periods (Figure 5), and these five variables also showed significant differences in the three periods. For HW days, HI was aggravated more by increased air temperature, and although the RH was relative lower, people still suffered from higher
155 apparent temperature than actual air temperature. During HW conditions, solar radiation reaching the ground heats the atmosphere increasing the near-surface temperature. Warmer air convection promotes atmospheric instability, with increased WS and higher BLH. It is clear that the meteorological variables during daytime HW periods were significantly different than under other conditions; and similarly, hourly O_3 concentrations under these conditions reached the peaks (Figure 5f). Therefore, it can be concluded that the difference in O_3 concentration was mainly due to meteorological conditions paired with
160 photochemical reactions in the boundary layer without considering O_3 emission precursors.

Moreover, the high temperatures on HW days not only brought a higher public risk related to high-temperature exposure, but also an increase in mortality related to O_3 exposure. Regardless of the type of stations, the O_3 and high-temperature stressful conditions suffered by the population during HW days has greatly increased. Specifically, for all stations, HWs have increased the ER caused by high temperatures and O_3 by 3.867% (90% CI: 3.863%, 3.875%) and 7.9% (90%CI: 0.78%, 15.78%),
165 respectively (Table 3). Interestingly, urbanization seems to have increased the ER induced by high temperatures over urban stations by 39.88%, but caused a 2.44% reduction in the ER associated with O_3. On the one hand, high temperatures and strong solar radiation during HW periods accelerate the rate of the photochemical reaction that produces O_3 (Pu et al., 2017; Sun et al., 2017), which is conducive to the production and accumulation of O_3. On the other hand, they increase the VOC emission of plants and contributes to the production of O_3 (Ma et al., 2019; Trainer et al., 1987; Wang et al., 2021a). The majority of
170 the isoprene emissions from forests in Beijing are mainly located in rural areas (Ma et al., 2019). Therefore, the O_3 concentrations over rural stations were higher than those over urban stations. In addition, the risk of O_3 exposure in the traffic stations was significantly lower than that of the urban and rural stations, and the risk of high-temperature exposure was slightly lower than that of urban stations. This has also led to the overall paired high-temperature and O_3 risk over traffic stations being lower than that over rural stations.

175 **3.2 Role of synoptic weather pattern and urbanization**

To further clarify the mechanism underlying the joint occurrence of HW–O_3 events in Beijing, three unfavourable synoptic weather patterns were identified as follows: (1) Type 1, characterized by the western Pacific subtropical high (WPSH) being located in the southeast of Beijing with prevailing southwesterly winds; (2) Type 2, controlled by a high-pressure system accompanied by weak southerly winds; and (3) Type 3, a low-vortex located over northeast Beijing with prevailing
180 northwesterly winds (Figures 6a–6c). Additionally, vertical cross-sections of the potential temperature and wind vectors at 1400 LST under the three patterns are shown in Figures 6e–6f. Under Type 1, low boundary layer paired with weak vertical motion favours pollutants' accumulation. Besides, the prevailing southwesterly wind may blow pollutants from the upwind direction to Beijing, and the northern mountains block the pollutants from continuing to be transported in the downward wind direction, causing the pollutants to gather in Beijing. For Type 2, a lower BLH and vertical convection together regulate the
185 transportation and accumulation of O_3 in the boundary layer. Under Type 3, there is a valley–plain wind circulation in the

boundary layer, and the strong downdraft over urban areas and the higher boundary layer cause the lowest MDA8 O_3 concentrations among the three weather types. Overall, Type 1 tends to be associated with the highest excess mortality caused by O_3, and Type 3 is related with the highest excess mortality caused by HWs. For excess mortality induced by the HW–O_3 compound events, Type 1 (12.59%) > Type 3 (12.05%) > Type 2 (11.66%). Although there is little difference in the HW–O_3

190 compound ER under the three weather types, the mechanisms of the three types are quite different. Under the modulation of weather circulation and boundary layer meteorological elements, Type 1, Type 2 and Type 3 were associated with high O_3 and intermediate T_{max} exposure, intermediate O_3 and low T_{max} exposure, and low O_3 and high T_{max} exposure (Figure 7), respectively. Therefore, the synoptic weather pattern plays an important role in regulating the formation mechanism of HW–O_3 compound events, which also further leads to it having a significant impact on morbidities and deaths caused by HW–O_3 compound events.

195 Table 4 also shows that there was an opposite urbanization regulation effect between high temperature and O_3 and their health risks under Type 1. In particular, HWs extended the urban–rural air temperature difference (the UHI effect) in Beijing (Table 2), as also found in our previous study (Zong et al., 2021b). It was mentioned earlier that the O_3 pollution in rural areas is higher than that in urban areas during HW periods. For Type 1, the strong southerly airflow caused the horizontal transportation of O_3 and its precursors from the southwest (urban) to the northeast (rural). Paired with the large number of forests in rural

200 areas during the HW that emitted additional VOCs (Ma et al., 2019), this further increased the difference in the O_3 concentration between urban and rural areas. Urbanization has a positive regulatory effect on the risk of heatwaves, but a negative one with respect to the risk of O_3. As for Type 2 and Type3, there was a little difference in O_3 exposure risk between urban and rural areas, but urban residents were more likely to be exposed to higher-temperature environment under Type 3 compared to Type 2. Specifically, the contribution rates of urbanization to the excessive mortality caused by high temperatures

205 and O_3 exposure were 27.72% and −2.58%, respectively, while the contribution rates of the synoptic pattern were 85.54% and 24.00%. In summary, urbanization and the synoptic pattern contributed 8.08% and 45% to the total HW–O_3 excess mortality (Table 5).

4 Discussions

In addition to heatstroke, heat exhaustion, heat fainting and heat cramps and other diseases, high temperature during HW days

210 can also lead to increased mortality of residents. Several studies have proposed that the mortality because of respiratory diseases, cardiovascular diseases and cardiopulmonary diseases induced by high temperature and O_3 exposure is particularly relevant (Chen et al., 2018; Du et al., 2020; Hu et al., 2019). Therefore, patients with pre-existing conditions as respiratory and cardiovascular diseases, should pay more attention and limit outdoor activity under heatwaves and O_3 polluted days. Furthermore, demographic, and socio-economic factors related to the level of urbanization, including age structure, education

215 and healthcare services, occupational types, and air-conditioning use, also greatly affect the exposure response function of high temperature and O_3. For instance, females, elderly and people with a lower degree of instruction have suffered significantly higher health risks from overexposure of high temperature and O_3 than the average population (Huang et al., 2015;

Yin et al., 2017; Zhang et al., 2017). However, this study mainly considers mortality by all-causes for all the population caused by high temperature and O_3 exposure. Health risks for high-risk groups such as the elderly, children, and patients with

220 cardiovascular and respiratory diseases should be higher than our results. Consequently, especially during synoptic weather patterns that can cause paired HW and O_3 pollution events, the responsible departments should strengthen the risk management of extreme compound events such as HW and O_3 pollution, establish an early warning system, configure emergency plans, strengthen the health precautions of respiratory and cardiovascular diseases, as well as the elderly and other vulnerable groups, and protect public health.

225 To date, there is no exact consensus on urbanization effects on risk of paired high temperature and O_3 exposure. Previously, a common perception was that urban residents were more prone to risks of heat effect in the context of global warming and UHI effect (Clarke, 1972; Goggins et al., 2012; Heaviside et al., 2017). Indeed, air temperature is one of the main reasons dominate the change in excess mortality caused by compound HW and O_3 events, In terms of the urban areas, the higher density of buildings, roads and population, greater heat capacity and anthropogenic heat, temperature of urban areas is significantly higher

230 than that of rural areas (Roth, 2007; Stewart & Oke, 2012). The heatwaves increase the urban and rural areas temperature difference, as well as the maximum temperature difference, so urban residents may expose to a higher temperature environment. However, the urban-rural difference in O_3 concentration modulated by HW days is inconsistent with that in temperature. Rural forests emit additional VOCs that generate O_3 during hot days (Ma et al., 2019; Wang et al., 2021a; Werner et al., 2020), resulting in O_3 pollution slightly lower in urban than rural areas(Gao et al., 2020a). Based on the regional exposure response

235 function model, urban areas suffer from higher mortality related to high temperature, while rural areas experience higher public mortality associated with O_3 pollution. It should be highlighted that also urbanization brought also some positive aspects. For example, a better economic level and medical conditions, can help to prevent more deaths to a certain extent; high air-conditioning utilization rate can also effectively reduce heat exposure; and the reduction in the proportion of highly exposed people engaged in agriculture, forestry and animal husbandry in urban areas also greatly reduces the risk of outdoor high-

240 temperature and O_3 overexposure. As a result, rural residents are more vulnerable to face the dual high temperature and O_3 stress, and their exposure response function coefficients may also be higher than that of urban residents (Hu et al., 2019; Kovach et al., 2015; Li et al., 2017; Williams et al., 2013; Xing et al., 2020; Zhang et al., 2017). This also means that under co-occurring heatwaves and ozone-polluted weather patterns, vulnerable groups in the suburbs should be warned on the risks of outdoor activity and limiting their exposure to the pollutants.

245 Regarding with the paired HW–O_3 events, though we moved a step forward in exploring role of synoptic weather pattern and urbanization, there are still some limitations in our study. As mentioned earlier, in a specific area, the health risks faced by residents adjusted by different levels of urbanization may be quite different. Moreover, the high temperature and O_3 compound health risk model for special populations (e.g., patients with cardiovascular and respiratory diseases, the elderly, children, etc.) can also be further established and analyzed. Therefore, in the future research on compound climate and pollution health

250 impacts it is necessary to consider a more refined discussion in a city based on the level of urbanization and among different population groups.

5 Conclusions

In this study, the complex mechanism of co-occurring HW–O_3 events in the boundary layer in Beijing was systematically investigated by combining meteorological observations, environmental monitoring observations, and reanalysis data, and the

255 regulatory role on health risks induced by such compound events was explained from the perspective of the synoptic pattern and urbanization.

The Beijing area not only experienced a stronger UHI effect during the summertime high-temperature HWs, but was also often accompanied by more serious O_3 pollution. In the period under study, the max temperature T_{max} and MDA8 O_3 concentrations during HW days were ~4.21℃ and ~37.98 μg m^{-3} higher than those on NHW days, respectively, excluding rainy daytime

260 days. When people are exposed to the dual stress of high temperatures and O_3 pollution on HW days, the increase in T_{max} and MDA8 O_3 concentrations is associated with an 11.78% (95% CI: 4.66%, 19.66%) higher excess mortality from all non-accidental causes. Three unfavourable synoptic weather patterns that dominate such compound events and were identified as: (1) Type 1, a high-pressure system located in the southeast of Beijing and accompanied by southwesterly winds, under which the weak downdraft and relative stable boundary layer weaken the vertical mixing of O_3 and induce heavy O_3 pollution,

265 consequently meaning that people consistently experience high health risks; (2) Type 2, in which Beijing is under the influence of a high-pressure system accompanied by weak southerly winds and sinking airflow in the boundary layer that favours O_3 transport together with its precursors. This translates into a lower excess mortality under Type 2 with respect to Type 1; and (3) Type 3, a low-pressure system located in the northeast of Beijing accompanied by northwesterly winds. Under this type, people endure stronger heat stress owing to higher temperatures and lower RH, but the higher BLH and large atmospheric

270 environment capacity alleviate O_3 exposure to a certain extent, which results in a decrease in O_3 concentration and ER compared with the other two patterns. Overall, the unfavourable weather types contributed ~45.76% to the excess mortality attributed to the HW–O_3 compound events.

In addition, urbanization has also exacerbated the combined health risks of high temperature and O_3 pollution, which contributed ~8.08%. During the co-occurring HW–O_3 days, urbanization greatly affected the increase in high temperatures

275 and related excess mortality risks in urban areas, which were significantly higher than those in rural areas. On the contrary, O_3 pollution and its health risks in urban areas were lower than those in rural areas, and the contribution of urbanization effects was negative. This is because those urban pollutants (O_3 and its precursors) were diffused and transported to the rural areas via local urban island circulation, which greatly increased the O_3 pollution and resultant excess mortality risk in rural areas, and reduced the O_3 concentration and related health risks in urban areas.

280 In summary, our findings help to better understand the formation mechanism of HW–O_3 compound events in Beijing, with robust supporting evidence from the perspective of synoptic patterns and urbanization. Our results also suggest that forecasting of identified synoptic patterns could help to avoid exposure of compound HW-O_3 events. However, the urbanization effect has an opposite regulatory effect on HWs and O_3, meaning that high temperatures and O_3 exposure is deserving of the establishment of a more refined health model that takes into account the differences between urban and rural areas.

Atmospheric
Chemistry
and Physics
Discussions

Data availability

The datasets that are analyzed and used to support the findings of this study are available in the public domains: The ground-level O3 observation data can be obtained from Beijing Municipal Ecological and Environmental Monitoring Center (http://www.bjmemc.com.cn/, last access on November 20, 2021). The hourly meteorological data can be obtained from the National Meteorological Information Center of the China Meteorological Administration (http://data.cma.cn/, last access on November 20, 2021). The ERA5 reanalysis data set is available at the European Centre for Medium-Range Weather Forecasts (https://cds.climate.copernicus.eu/cdsapp#!/home, last access on November 20, 2021).

Competing interests

The authors declare that they have no conflict of interests.

Author contributions

L. Zong: Methodology, Data Curation, Formal Analysis, Writing- Original draft preparation, Results Discussion, Writing-Reviewing and Editing; Y. Yang, H. Xia: Conceptualization, Methodology, Formal Analysis, Results Discussion, Writing-Reviewing and Editing; Z. Sun, Z. Zheng, X. Li, G. Ning, Y. Li, Z. Gao, S. Lolli: Results Discussion, Comments, Writing-Reviewing and Editing.

Acknowledgments

References

Atkinson, R. W., Yu, D., Armstrong, B. G., Pattenden, S., Wilkinson, P., Doherty, R. M., Heal, M. R. and Anderson, H. R.: Results from Five Urban and Five Rural U . K . Populations, Environ. Health Perspect., 120(10), 1411–1417, 2012.

Cao, R., Wang, Y., Huang, J., Zeng, Q., Pan, X., Li, G. and He, T.: The construction of the air quality health index (AQHI) and a validity comparison based on three different methods, Environ. Res., 197(March), 110987, doi:10.1016/j.envres.2021.110987, 2021.

Chen, R., Yin, P., Wang, L., Liu, C., Niu, Y., Wang, W., Jiang, Y., Liu, Y., Liu, J., Qi, J., You, J., Kan, H. and Zhou, M.: Association between ambient temperature and mortality risk and burden: Time series study in 272 main Chinese cities, BMJ, 363(k4306), doi:10.1136/bmj.k4306, 2018.

310   Chew, L. W., Liu, X., Li, X. X. and Norford, L. K.: Interaction between heat wave and urban heat island: A case study in a
        tropical coastal city, Singapore, Atmos. Res., 247(2020), 105134, doi:10.1016/j.atmosres.2020.105134, 2021.

        Clarke, J. F.: Some effects of the urban structure on heat mortality, Environ. Res., 5(1), 93–104, doi:10.1016/0013-
        9351(72)90023-0, 1972.

        Dou, J., Wang, Y., Bornstein, R. and Miao, S.: Observed spatial characteristics of Beijing urban climate impacts on summer
315   thunderstorms, J. Appl. Meteorol. Climatol., 54(1), 94–105, doi:10.1175/JAMC-D-13-0355.1, 2015.

        Du, X., Chen, R., Meng, X., Liu, C., Niu, Y., Wang, W., Li, S., Kan, H. and Zhou, M.: The establishment of National Air
        Quality Health Index in China, Environ. Int., 138(2019), 105594, doi:10.1016/j.envint.2020.105594, 2020.

        Fan, H., Zhao, C. and Yang, Y.: A comprehensive analysis of the spatio-temporal variation of urban air pollution in China
        during 2014–2018, Atmos. Environ., 220, 117066, doi:10.1016/j.atmosenv.2019.117066, 2020.

320   Gao, L., Yue, X., Meng, X., Du, L., Lei, Y., Tian, C. and Qiu, L.: Comparison of Ozone and PM2.5 Concentrations over
        Urban, Suburban, and Background Sites in China, Adv. Atmos. Sci., 37(12), 1297–1309, doi:10.1007/s00376-020-0054-2,
        2020a.

        Gao, M., Gao, J., Zhu, B., Kumar, R., Lu, X., Song, S., Zhang, Y. and Jia, B.: Ozone pollution over China and India :
        seasonality and sources, , 2000, 4399–4414, 2020b.

325   Goggins, W. B., Chan, E. Y. Y., Ng, E., Ren, C. and Chen, L.: Effect modification of the association between short-term
        meteorological factors and mortality by urban heat islands in Hong Kong, PLoS One, 7(6), e38511,
        doi:10.1371/journal.pone.0038551, 2012.

        Gu, Y., Wong, T. W., Law, S., Dong, G., Ho, K. F., Yang, Y. and Yim, S. H. L.: Impacts of sectoral emissions in China and
        the implications: Air quality, public health, crop production, and economic costs, Environ. Res. Lett., 13, doi:10.1088/1748-
330   9326/aad138, 2018.

        Han, H., Liu, J., Shu, L., Wang, T. and Yuan, H.: Local and synoptic meteorological influences on daily variability in
        summertime surface ozone in eastern China, Atmos. Chem. Phys., 20(1), 203–222, doi:10.5194/acp-20-203-2020, 2020.

        Heaviside, C., Macintyre, H. and Vardoulakis, S.: The Urban Heat Island: Implications for Health in a Changing
        Environment, Curr. Environ. Heal. reports, 4(3), 296–305, doi:10.1007/s40572-017-0150-3, 2017.

335   Herring, S. C., Christidis, N., Hoell, A., Hoerling, M. P. and Stott, P. A.: Explaining Extreme Events of 2017 from a Climate
        Perspective, Bull. Am. Meteorol. Soc., 100(1), S1–S117, doi:10.1175/BAMS-ExplainingExtremeEvents2017.1, 2019.

        Hertig, E., Russo, A. and Trigo, R. M.: Heat and ozone pollution waves in central and south Europe—characteristics,
        weather types, and association with mortality, Atmosphere (Basel)., 11(12), 1–18, doi:10.3390/atmos11121271, 2020.

        Hu, K., Guo, Y., Hochrainer-Stigler, S., Liu, W., See, L., Yang, X., Zhong, J., Fei, F., Chen, F., Zhang, Y., Zhao, Q., Chen,
340   G., Chen, Q., Zhang, Y., Ye, T., Ma, L., Li, S. and Qi, J.: Evidence for urban–rural disparity in temperature–mortality
        relationships in Zhejiang Province, China, Environ. Health Perspect., 127(3), 1–11, doi:10.1289/EHP3556, 2019.

Atmospheric
Chemistry
and Physics
Discussions

Huang, Z., Lin, H., Liu, Y., Zhou, M., Liu, T., Xiao, J., Zeng, W., Li, X., Zhang, Y., Ebi, K. L., Tong, S., Ma, W. and Wang, L.: Individual-level and community-level effect modifiers of the temperature-mortality relationship in 66 Chinese communities, BMJ Open, 5(9), doi:10.1136/bmjopen-2015-009172, 2015.

345 Jiang, S., Lee, X., Wang, J. and Wang, K.: Amplified Urban Heat Islands during Heat Wave Periods, J. Geophys. Res. Atmos., 124(14), 7797–7812, doi:10.1029/2018JD030230, 2019.

Katsouyanni, K., Pantazopoulou, A., Touloumi, G., Tselepidaki, I. and Moustris, K.: Archives of Environmental Health : An International Evidence for Interaction between Air Pollution and High Temperature in the Causation of Excess Mortality Evidence for Interaction between Air Pollution and High Temperature in the Causation of Excess Mor, Arch. Environ. Heal.

350 An Int. J., 48(4), 235–242, doi:10.1080/00039896.1993.9940365, 1993.

Kovach, M. M., Konrad, C. E. and Fuhrmann, C. M.: Area-level risk factors for heat-related illness in rural and urban locations across North Carolina, USA, Appl. Geogr., 60, 175–183, doi:10.1016/j.apgeog.2015.03.012, 2015.

Lehner, F., Deser, C. and Sanderson, B. M.: Future risk of record-breaking summer temperatures and its mitigation, Clim. Change, 146(3–4), 363–375, doi:10.1007/s10584-016-1616-2, 2018.

355 Lelieveld, J., Hadjinicolaou, P., Kostopoulou, E., Giannakopoulos, C., Pozzer, A., Tanarhte, M. and Tyrlis, E.: Model projected heat extremes and air pollution in the eastern Mediterranean and Middle East in the twenty-first century, Reg. Environ. Chang., 14(5), 1937–1949, doi:10.1007/s10113-013-0444-4, 2014.

Li, D., Sun, T., Liu, M., Yang, L., Wang, L. and Gao, Z.: Contrasting responses of urban and rural surface energy budgets to heat waves explain synergies between urban heat islands and heat waves, Environ. Res. Lett., 10(5), 1–10,

360 doi:10.1088/1748-9326/10/5/054009, 2015.

Li, K., Jacob, D. J., Liao, H., Shen, L., Zhang, Q. and Bates, K. H.: Anthropogenic drivers of 2013–2017 trends in summer surface ozone in China, Proc. Natl. Acad. Sci. U. S. A., 116(2), 422–427, doi:10.1073/pnas.1812168116, 2019.

Li, Y., Odame, E. A., Silver, K. and Zheng, S.: Comparing Urban and Rural Vulnerability to Heat-Related Mortality: A Systematic Review and Meta-analysis, J. Glob. Epidemiol. Environ. Heal., 1(1), 9–15, doi:10.29199/geeh.101016, 2017.

365 Liu, J., Ai, S., Qi, J., Wang, L., Zhou, M., Wang, C., Yin, P. and Lin, H.: Defining region-specific heatwave in China based on a novel concept of "avoidable mortality for each temperature unit decrease," Adv. Clim. Chang. Res., 12(5), 611–618, doi:10.1016/j.accre.2021.08.002, 2021.

Liu, N., Zhou, S., Liu, C. and Guo, J.: Synoptic circulation pattern and boundary layer structure associated with PM2.5 during wintertime haze pollution episodes in Shanghai, Atmos. Res., 228(46), 186–195, doi:10.1016/j.atmosres.2019.06.001,

370 2019.

Luo, M. and Lau, N. C.: Increasing Heat Stress in Urban Areas of Eastern China: Acceleration by Urbanization, Geophys. Res. Lett., 45(23), 13,060-13,069, doi:10.1029/2018GL080306, 2018.

Luo, M. and Lau, N. C.: Urban Expansion and Drying Climate in an Urban Agglomeration of East China, Geophys. Res. Lett., 46(12), 6868–6877, doi:10.1029/2019GL082736, 2019.

375 Ma, M., Gao, Y., Wang, Y., Zhang, S., Ruby Leung, L., Liu, C., Wang, S., Zhao, B., Chang, X., Su, H., Zhang, T., Sheng, L., Yao, X. and Gao, H.: Substantial ozone enhancement over the North China Plain from increased biogenic emissions due to heat waves and land cover in summer 2017, Atmos. Chem. Phys., 19(19), 12195–12207, doi:10.5194/acp-19-12195-2019, 2019.

Ma, W., Zeng, W., Zhou, M., Wang, L., Rutherford, S., Lin, H., Liu, T., Zhang, Y., Xiao, J., Zhang, Y., Wang, X., Gu, X.
380 and Chu, C.: The short-term effect of heat waves on mortality and its modifiers in China: An analysis from 66 communities, Environ. Int., 75, 103–109, doi:10.1016/j.envint.2014.11.004, 2015.

Meehl, G. A. and Tebaldi, C.: More Intense , More Frequent , and Longer Lasting Heat Waves in the 21st Century, Science (80-.)., 305(5686), 994–997, doi:10.1126/science.1098704, 2004.

Meehl, G. A., Arblaster, J. M. and Tebaldi, C.: Contributions of natural and anthropogenic forcing to changes in temperature
385 extremes over the United States, Geophys. Res. Lett., 34(August), 1–5, doi:10.1029/2007GL030948, 2007.

Miao, Y., Liu, S. and Huang, S.: Synoptic pattern and planetary boundary layer structure associated with aerosol pollution during winter in Beijing, China, Sci. Total Environ., 682, 464–474, doi:10.1016/j.scitotenv.2019.05.199, 2019.

Ngarambe, J., Nganyiyimana, J., Kim, I., Santamouris, M. and Young Yun, G.: Synergies between urban heat island and heat waves in Seoul: The role of wind speed and land use characteristics, PLoS One, 15(12 December),
390 doi:10.1371/journal.pone.0243571, 2020.

Ning, G., Yim, S. H. L., Wang, S., Duan, B., Nie, C., Yang, X., Wang, J. and Shang, K.: Synergistic effects of synoptic weather patterns and topography on air quality: a case of the Sichuan Basin of China, Clim. Dyn., 53(11), 6729–6744, doi:10.1007/s00382-019-04954-3, 2019.

Ning, G., Yim, S. H. L., Yang, Y., Gu, Y. and Dong, G.: Modulations of synoptic and climatic changes on ozone pollution
395 and its health risks in mountain-basin areas, Atmos. Environ., 240, 117808, doi:10.1016/j.atmosenv.2020.117808, 2020.

Oke, T. R. and Maxwell, G. B.: Urban heat island dynamics in Montreal and Vancouver, Atmos. Environ., 9(2), 191–200, doi:10.1016/0004-6981(75)90067-0, 1975.

Pattenden, S., Armstrong, B., Milojevic, A., Heal, M. R., Chalabi, Z., Doherty, R., Barratt, B., Kovats, R. S., Wilkinson, P., Pattenden, S., Armstrong, B., Milojevic, A., Heal, M. R., Chalabi, Z., Doherty, R., Barratt, B., Kovats, R. S. and Wilkinson,
400 P.: Ozone , heat and mortality : acute effects in 15 British conurbations, Occup. Environ. Med., 67(10), 699–707, doi:10.1136/oem.2009.051714, 2010.

Patz, J. A., Campbell-Lendrum, D., Holloway, T. and Foley, J. A.: Impact of regional climate change on human health, Nature, 438(7066), 310–317, doi:10.1038/nature04188, 2005.

Pope, R. J., Butt, E. W., Chipperfield, M. P., Doherty, R. M., Fenech, S., Schmidt, A., Arnold, S. R. and Savage, N. H.: The
405 impact of synoptic weather on UK surface ozone and implications for premature mortality, Environ. Res. Lett., 11(12), doi:10.1088/1748-9326/11/12/124004, 2016.

Pu, X., Wang, T. J., Huang, X., Melas, D., Zanis, P., Papanastasiou, D. K. and Poupkou, A.: Enhanced surface ozone during the heat wave of 2013 in Yangtze River Delta region, China, Sci. Total Environ., 603–604, 807–816, doi:10.1016/j.scitotenv.2017.03.056, 2017.

410   Rastogi, D.: Revisiting Recent U . S . Heat Waves in a Warmer and More Humid Climate, Geophys. Res. Lett., 47(9), 1–11, doi:10.1029/2019GL086736, 2020.

Ren, G. Y., Chu, Z. Y., Chen, Z. H. and Ren, Y. Y.: Implications of temporal change in urban heat island intensity observed at Beijing and Wuhan stations, Geophys. Res. Lett., 34(5), 1–5, doi:10.1029/2006GL027927, 2007.

Rizwan, A. M., DENNIS, L. Y. C. and LIU, C.: A review on the generation, determination and mitigation of Urban Heat

415   Island, J. Environ. Sci., 20(1), 120–128, doi:10.1016/S1001-0742(08)60019-4, 2008.

Roth, M.: Review of urban climate research in (sub)tropical regions, Int. J. Climatol., 27, 1859–1837, doi:10.1002/joc.1591, 2007.

Rothfusz, L.: The heat index equation, Natl. Weather Serv. Tech. Attach., SR:23-90 [online] Available from: https://www.weather.gov/media/ffc/ta_htindx .PDF., 1990.

420   Sartor, F., Rene, S., Claude, D. and Denise, W.: Temperature, ambient ozone levels, and mortality during summer, 1994, in Belgium, Environ. Res., 70, 105–113, doi:10.1006/enrs.1995.1054, 1995.

Shu, L., Xie, M., Wang, T., Gao, D., Chen, P., Han, Y., Li, S., Zhuang, B. and Li, M.: Integrated studies of a regional ozone pollution synthetically affected by subtropical high and typhoon system in the Yangtze River Delta region, China, Atmos. Chem. Phys., 16(24), 15801–15819, doi:10.5194/acp-16-15801-2016, 2016.

425   Stewart, I. D. and Oke, T. R.: Local climate zones for urban temperature studies, Bull. Am. Meteorol. Soc., 93(12), 1879–1900, doi:10.1175/BAMS-D-11-00019.1, 2012.

Sun, W., Hess, P. and Liu, C.: The impact of meteorological persistence on the distribution and extremes of ozone, Geophys. Res. Lett., 44(3), 1545–1553, doi:10.1002/2016GL071731, 2017.

Tan, J., Zheng, Y., Tang, X., Guo, C., Li, L., Song, G., Zhen, X., Yuan, D., Kalkstein, A. J., Li, F. and Chen, H.: The urban

430   heat island and its impact on heat waves and human health in Shanghai, Int. J. Biometeorol., 54(1), 75–84, doi:10.1007/s00484-009-0256-x, 2010.

Trainer, M., Williams, E., Parrish, D., Buhr, M., Allwine, E., Westberg, H., Fehsenfeld, F. and Liu, S.: Models and observations of the impact of natural hydrocarbons on rural ozone, Nature, 329(6164), 705–707, doi:10.1038/329705a0, 1987.

435   Wang, H., Wu, K., Liu, Y., Sheng, B., Lu, X., He, Y., Xie, J., Wang, H. and Fan, S.: Role of Heat Wave-Induced Biogenic VOC Enhancements in Persistent Ozone Episodes Formation in Pearl River Delta, J. Geophys. Res. Atmos., 126(12), 1–19, doi:10.1029/2020JD034317, 2021a.

Wang, J., Chen, Y., Liao, W., He, G., Tett, S. F. B., Yan, Z., Zhai, P., Feng, J., Ma, W., Huang, C. and Hu, Y.: Anthropogenic emissions and urbanization increase risk of compound hot extremes in cities, Nat. Clim. Chang.,

440   doi:10.1038/s41558-021-01196-2, 2021b.

Wang, K., Wang, J., Wang, P., Sparrow, M., Yang, J. and Chen, H.: Influences of urbanization on surface characteristics as derived from the Moderate-Resolution Imaging Spectroradiometer: A case study for the Beijing metropolitan area, J. Geophys. Res. Atmos., 112(22), 1–12, doi:10.1029/2006JD007997, 2007.

Wang, K., Jiang, S., Wang, J., Zhou, C., Wang, X. and Lee, X.: Comparing the diurnal and seasonal variabilities of atmospheric and surface urban heat islands based on the Beijing urban meteorological network, J. Geophys. Res., 122(4), 2131–2154, doi:10.1002/2016JD025304, 2017.

Wang, N., Lyu, X., Deng, X., Huang, X., Jiang, F. and Ding, A.: Aggravating O 3 pollution due to NO x emission control in eastern China, Sci. Total Environ., 677(x), 732–744, doi:10.1016/j.scitotenv.2019.04.388, 2019.

Wang, Y., Wild, O., Chen, X., Wu, Q., Gao, M., Chen, H., Qi, Y. and Wang, Z.: Health impacts of long-term ozone exposure in China over 2013–2017, Environ. Int., 144, 106030, doi:10.1016/j.envint.2020.106030, 2020.

Werner, C., Fasbender, L., Romek, K. M., Yáñez-Serrano, A. M. and Kreuzwieser, J.: Heat Waves Change Plant Carbon Allocation Among Primary and Secondary Metabolism Altering CO2 Assimilation, Respiration, and VOC Emissions, Front. Plant Sci., 11(August), 1–17, doi:10.3389/fpls.2020.01242, 2020.

Williams, S., Bi, P., Newbury, J., Robinson, G., Pisaniello, D., Saniotis, A. and Hansen, A.: Extreme heat and health: Perspectives from health service providers in rural and remote communities in South Australia, Int. J. Environ. Res. Public Health, 10(11), 5565–5583, doi:10.3390/ijerph10115565, 2013.

Wong, T. W., Tam, W. W. S., Yu, I. T. S., Lau, A. K. H., Pang, S. W. and Wong, A. H. S.: Developing a risk-based air quality health index, Atmos. Environ., 76, 52–58, doi:10.1016/j.atmosenv.2012.06.071, 2013.

Xing, Q., Sun, Z. Bin, Tao, Y., Zhang, X., Miao, S., Zheng, C. and Tong, S.: Impacts of urbanization on the temperature-cardiovascular mortality relationship in Beijing, China, Environ. Res., 191, 110234, doi:10.1016/j.envres.2020.110234, 2020.

Xu, Z., Fitzgerald, G., Guo, Y., Jalaludin, B. and Tong, S.: Impact of heatwave on mortality under different heatwave definitions : A systematic review and meta-analysis, Environ. Int., 89–90, 193–203, doi:10.1016/j.envint.2016.02.007, 2016.

Yang, P., Ren, G. and Liu, W.: Spatial and temporal characteristics of Beijing urban heat island intensity, J. Appl. Meteorol. Climatol., 52(8), 1803–1816, doi:10.1175/JAMC-D-12-0125.1, 2013.

Yang, X., Ruby Leung, L., Zhao, N., Zhao, C., Qian, Y., Hu, K., Liu, X. and Chen, B.: Contribution of urbanization to the increase of extreme heat events in an urban agglomeration in east China, Geophys. Res. Lett., 44(13), 6940–6950, doi:10.1002/2017GL074084, 2017.

Yang, Y., Zheng, X., Gao, Z., Wang, H., Wang, T., Li, Y., Lau, G. N. C. and Yim, S. H. L.: Long-Term Trends of Persistent Synoptic Circulation Events in Planetary Boundary Layer and Their Relationships With Haze Pollution in Winter Half Year Over Eastern China, J. Geophys. Res. Atmos., 123(19), 10,991-11,007, doi:10.1029/2018JD028982, 2018.

Yang, Y., Zheng, Z., Yim, S. Y. L., Roth, M., Ren, G., Gao, Z., Wang, T., Li, Q., Shi, C., Ning, G. and Li, Y.: PM2.5 Pollution Modulates Wintertime Urban Heat Island Intensity in the Beijing-Tianjin-Hebei Megalopolis, China, Geophys. Res. Lett., 47(1), 1–12, doi:10.1029/2019GL084288, 2020.

475 Yang, Y., Wang, R., Chen, F., Liu, C., Bi, X. and Huang, M.: Synoptic weather patterns modulate the frequency, type and vertical structure of summer precipitation over Eastern China: A perspective from GPM observations, Atmos. Res., 249, doi:10.1016/j.atmosres.2020.105342, 2021.

Yim, S. H. L., Wang, M., Gu, Y., Yang, Y., Dong, G. and Li, Q.: Effect of Urbanization on Ozone and Resultant Health Effects in the Pearl River Delta Region of China, J. Geophys. Res. Atmos., 124(21), 11568–11579,

480 doi:10.1029/2019JD030562, 2019.

Yin, P., Chen, R., Wang, L., Meng, X., Liu, C., Niu, Y., Lin, Z., Liu, Y., Liu, J., Qi, J., You, J., Zhou, M. and Kan, H.: Ambient ozone pollution and daily mortality: A nationwide study in 272 Chinese cities, Environ. Health Perspect., 125(11), 1–7, doi:10.1289/EHP1849, 2017.

Yu, M., Liu, Y., Dai, Y. and Yang, A.: Impact of urbanization on boundary layer structure in Beijing, Clim. Change, 120(1–

485 2), 123–136, doi:10.1007/s10584-013-0788-2, 2013.

Yu, S., Yin, S., Zhang, R., Wang, L., Su, F., Zhang, Y. and Yang, J.: Spatiotemporal characterization and regional contributions of O3 and NO2: An investigation of two years of monitoring data in Henan, China, J. Environ. Sci. (China), 90(November), 29–40, doi:10.1016/j.jes.2019.10.012, 2020.

Zanis, P., Monks, P. S., Schuepbach, E., Carpenter, L. J., Green, T. J., Mills, G. P., Bauguitte, S. and Penkett, S. A.: In situ

490 ozone production under free tropospheric conditions during FREETEX '98 in the Swiss Alps, J. Geophys. Res. - Atmos., 105, 24223–24234, 2000.

Zanis, P., Katragkou, E., Tegoulias, I., Poupkou, A., Melas, D., Huszar, P. and Giorgi, F.: Evaluation of near surface ozone in air quality simulations forced by a regional climate model over Europe for the period 1991-2000, Atmos. Environ., 45, 6489–6500, doi:10.1016/j.atmosenv.2011.09.001, 2011.

495 Zhang, W. and Villarini, G.: On the weather types that shape the precipitation patterns across the U.S. Midwest, Clim. Dyn., 53(7–8), 4217–4232, doi:10.1007/s00382-019-04783-4, 2019.

Zhang, Y., Yu, C., Bao, J. and Li, X.: Impact of temperature on mortality in Hubei, China: A multi-county time series analysis, Sci. Rep., 7, 45093, doi:10.1038/srep45093, 2017.

Zhang, Z., Zhang, X., Gong, D., Quan, W., Zhao, X., Ma, Z. and Kim, S. J.: Evolution of surface O3 and PM2.5

500 concentrations and their relationships with meteorological conditions over the last decade in Beijing, Atmos. Environ., 108, 67–75, doi:10.1016/j.atmosenv.2015.02.071, 2015.

Zhao, Z. and Wang, Y.: Influence of the West Pacific subtropical high on surface ozone daily variability in summertime over eastern China, Atmos. Environ., 170, 197–204, doi:10.1016/j.atmosenv.2017.09.024, 2017.

Zheng, Z., Ren, G., Wang, H., Dou, J., Gao, Z., Duan, C., Li, Y., Ngarukiyimana, J. P., Zhao, C., Cao, C., Jiang, M. and

505 Yang, Y.: Relationship Between Fine-Particle Pollution and the Urban Heat Island in Beijing, China: Observational Evidence, Boundary-Layer Meteorol., 169(1), 93–113, doi:10.1007/s10546-018-0362-6, 2018.

Zheng, Z., Zhao, C., Lolli, S., Wang, X., Wang, Y., Ma, X., Li, Q. and Yang, Y.: Diurnal variation of summer precipitation modulated by air pollution: Observational evidences in the beijing metropolitan area, Environ. Res. Lett., 15(9), doi:10.1088/1748-9326/ab99fc, 2020.

510 Zinzi, M., Agnoli, S., Burattini, C. and Mattoni, B.: On the thermal response of buildings under the synergic effect of heat waves and urban heat island, Sol. Energy, 211, 1270–1282, doi:10.1016/j.solener.2020.10.050, 2020.

Zong, L., Yang, Y., Gao, M., Wang, H., Wang, P., Zhang, H., Wang, L., Ning, G., Liu, C., Li, Y. and Gao, Z.: Large-scale synoptic drivers of co-occurring summertime ozone and PM2.5 pollution in eastern China, Atmos. Chem. Phys., 21, 9105–9124, doi:10.5194/acp-21-9105-2021, 2021a.

515 Zong, L., Liu, S., Yang, Y., Ren, G., Yu, M., Zhang, Y. and Li, Y.: Synergistic Influence of Local Climate Zones and Wind Speeds on the Urban Heat Island and Heat Waves in the Megacity of Beijing, China, Front. Earth Sci., 9, 458, doi:10.3389/feart.2021.673786, 2021b.

520
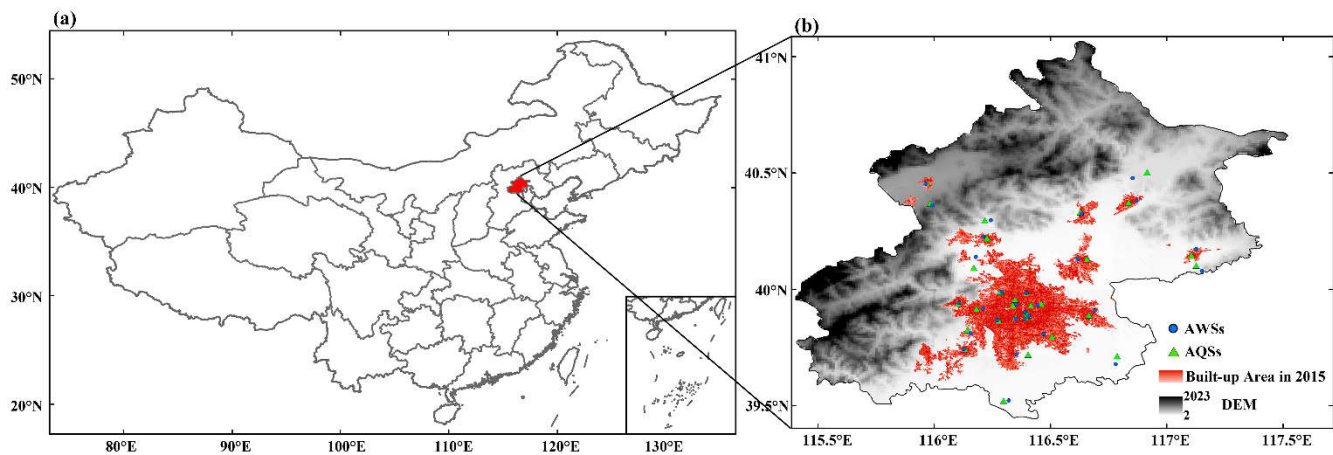
Figure 1: (a) Geography of Beijing. (b) Distribution of AWSs and air quality stations (AQSs) in Beijing (superimposed on the built-up area data for 2015 from digital elevation model data).
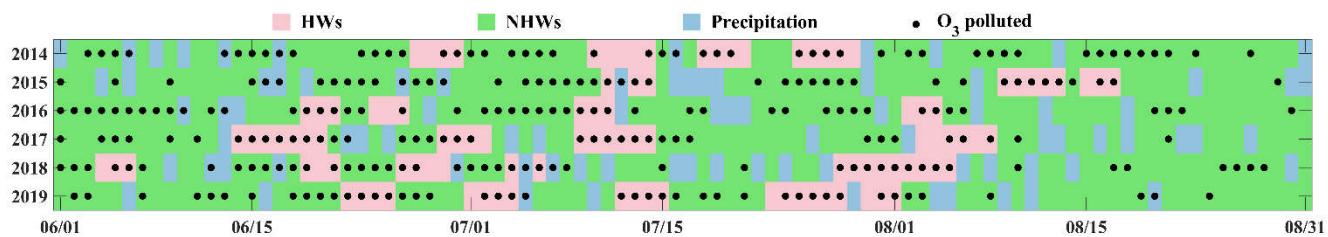
525 **Figure 2: Time series of weather types, in which the black dots indicate O₃ pollution that occurred on that day.**

Atmospheric
Chemistry
and Physics
Discussions
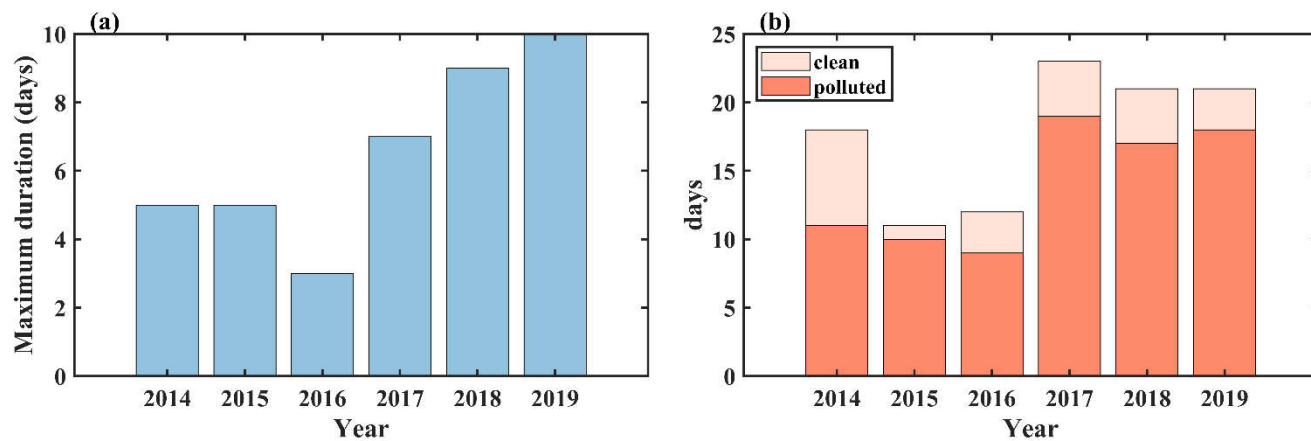
Figure 3: (a) Maximum number of days of HW events each year. (b) Proportion of O₃ pollution during HW events each year.

530
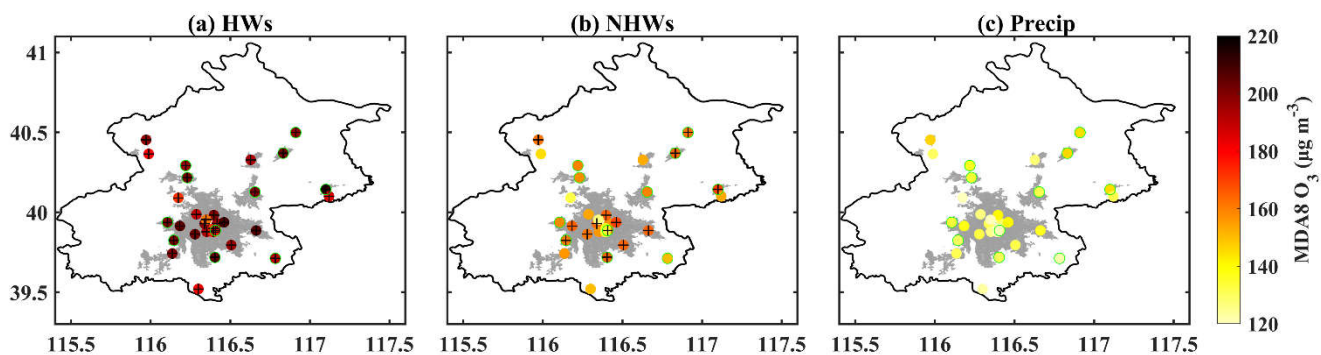
Figure 4: Distribution of MDA8 O₃ under (a) HWs, (b) NHWs, and (c) precipitation periods (superimposed on built-up area data for 2015, with green dots indicating vegetation covered stations). The diurnal variation of (d) air temperature, (e) RH, (f) HI, (g) BLH, (h) WS and (i) O₃, under HWs, NHWs and precipitation periods (shading indicates standard deviation).

535
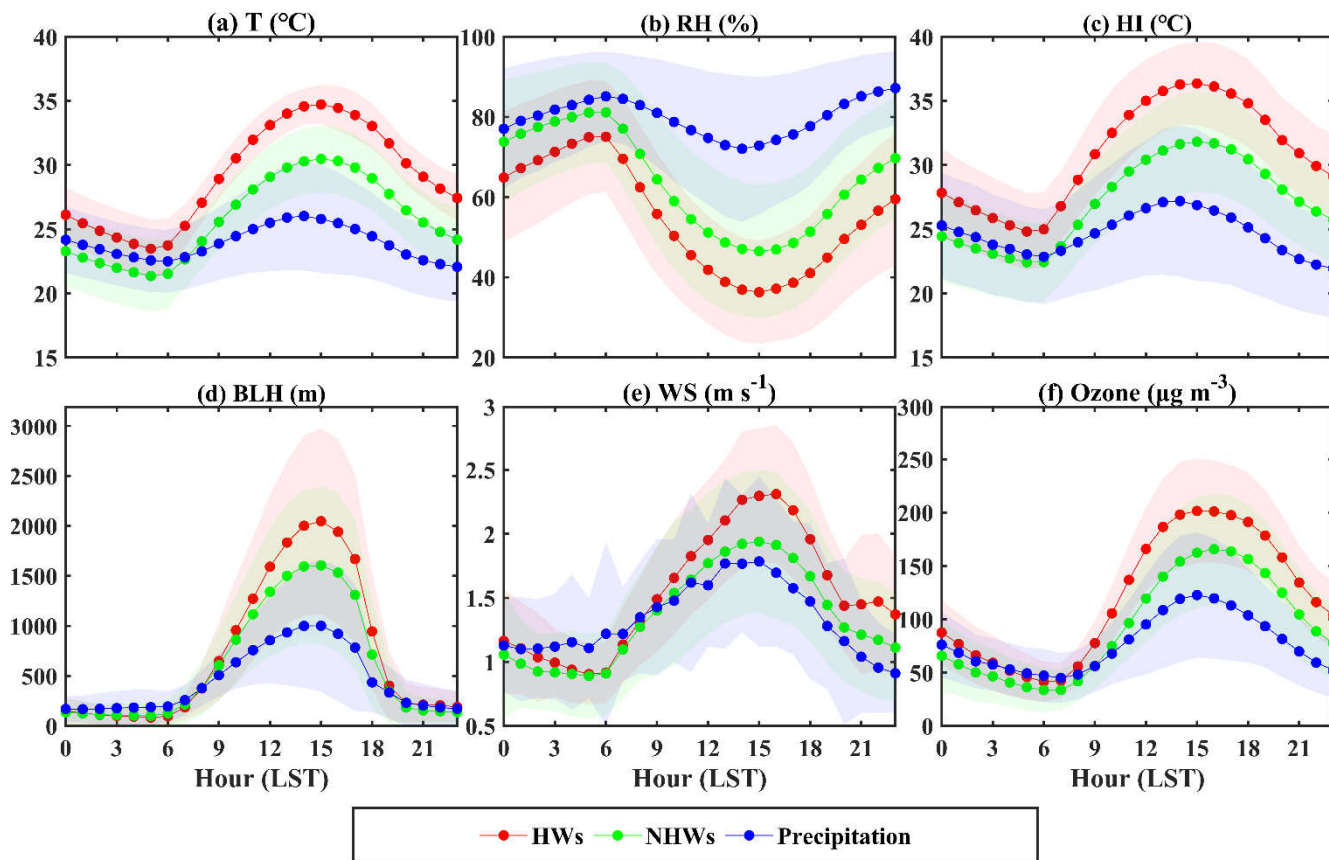
Figure 5: The diurnal variation of (a) air temperature, (b) RH, (c) HI, (d) BLH, (e) WS and (f) O₃, under HWs, NHWs and precipitation periods (shading indicates standard deviation).

540
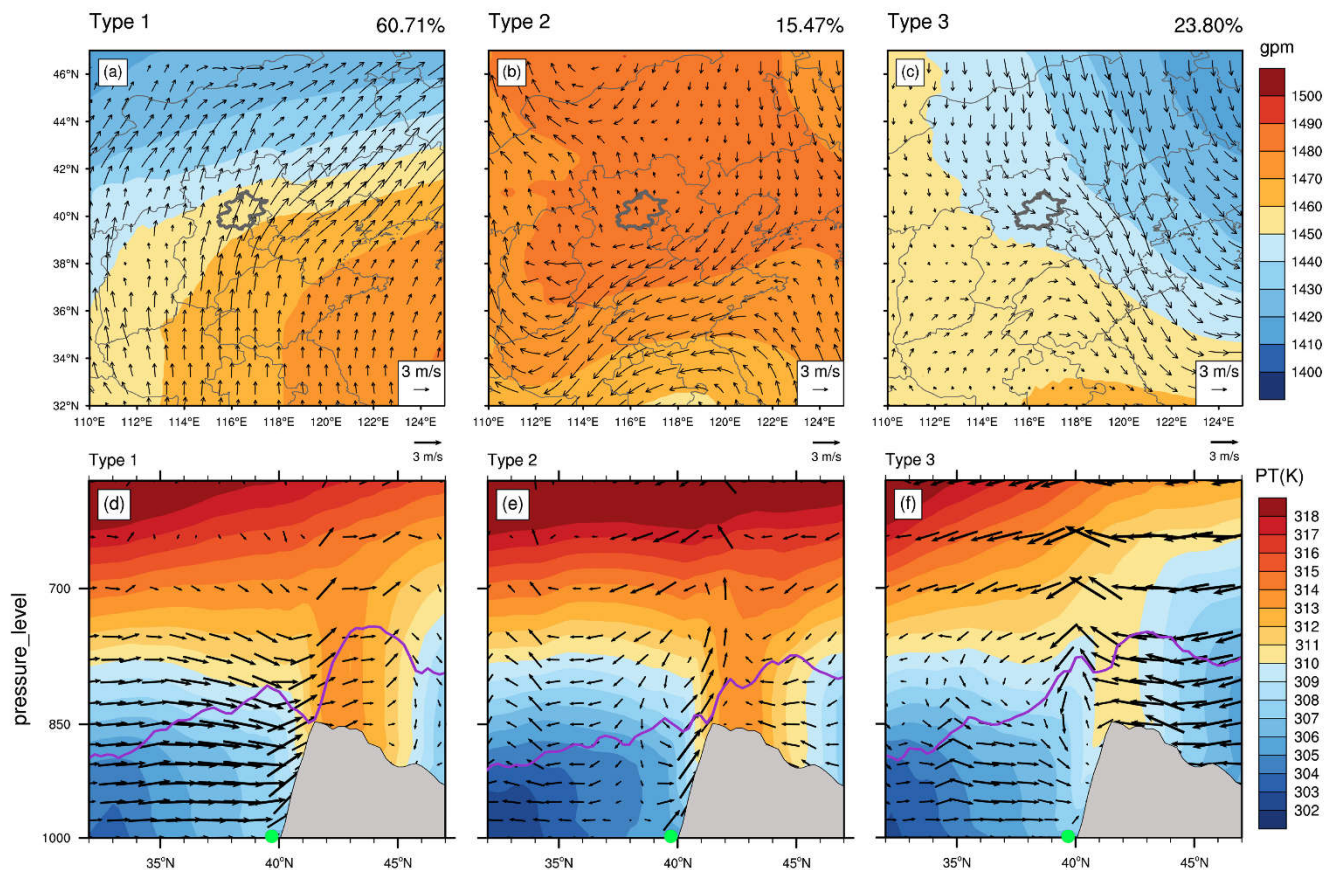
Figure 6: (a–c) 850-hPa GH (contours) and υv-wind (vectors) patterns related to HWs and O$_3$ pollution compound events based on objective classification (grey outline represents Beijing, and the number in the upper-right corner of each panel indicates the frequency of occurrence of each pattern). (d–f) Vertical cross-sections of the potential temperature (contours) and wind vectors (synthesized by v and scaled ω, ω scaled by 100) averaged between 116.0°E and 117.0°E associated with the synoptic patterns (purple solid lines mark the BLH, black contours mark the topography, and the green dot marks the location of Beijing).

Atmospheric
Chemistry
and Physics
Discussions

Open Access

EGU
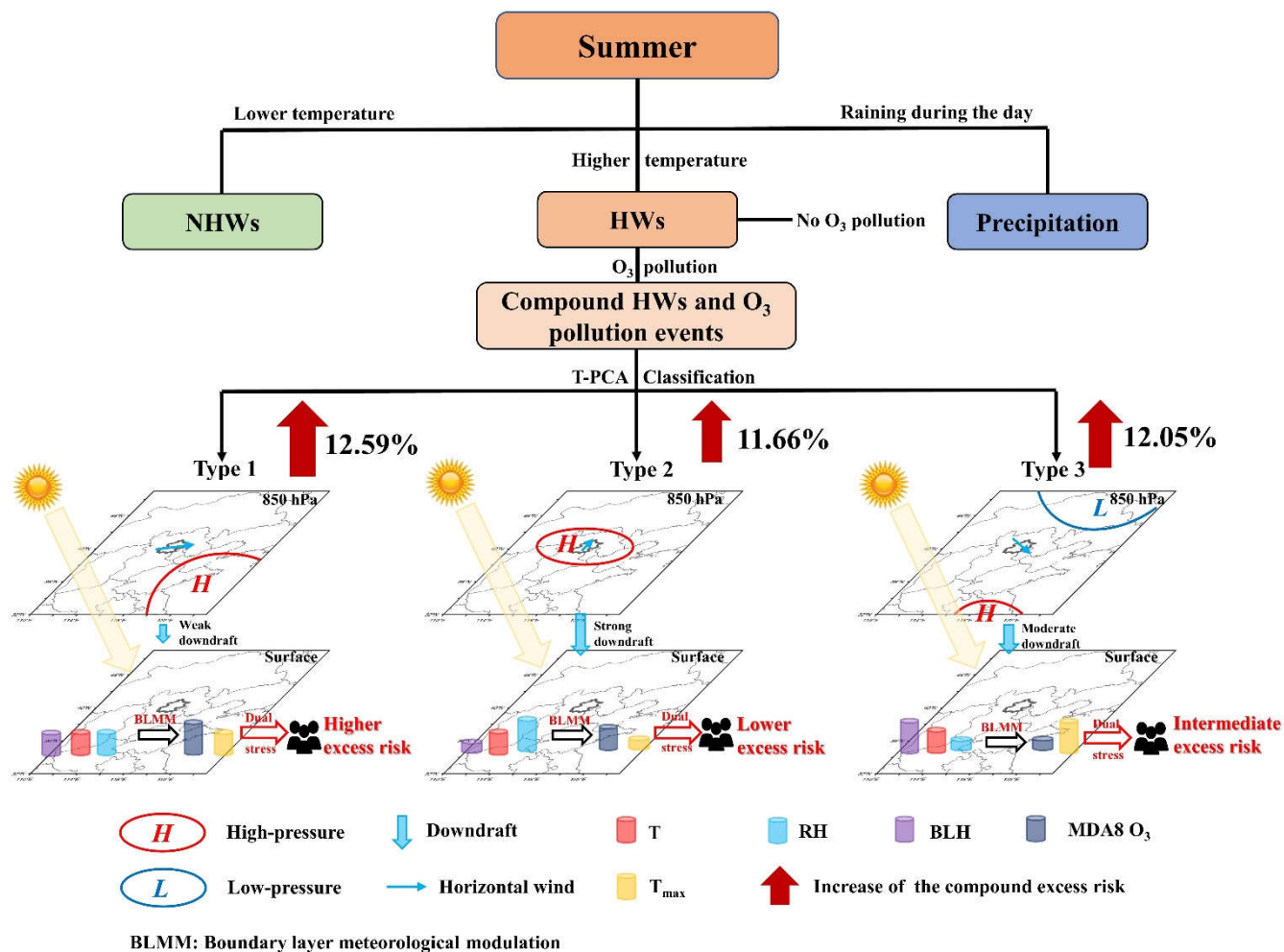
Figure 7: Schematic illustration of the mechanism of HW and O₃ compound pollution events under different synoptic weather patterns (height of the icon indicates the size of each variable).

Table 1: The location information and station type of AQSs, the corresponding AWSs are the closest matching weather station among 295 AWSs.

AQI Station	Lon (°)	Lat (°)	Type	AWS	Lon (°)	Lat (°)
DS	116.42	39.93	Urban	A1003	116.44	39.93
TT	116.41	39.89	Urban*	A1016	116.41	39.88
GY	116.34	39.93	Urban	A1006	116.35	39.93
WSXG	116.35	39.88	Urban	A1015	116.35	39.87
ATZX	116.40	39.98	Urban	A1007	116.40	39.98
NZG	116.46	39.94	Urban	A1003	116.44	39.93
WL	116.29	39.99	Urban	54399	116.29	39.99
BBXQ	116.17	40.09	Urban	A1033	116.18	40.14
FTHY	116.28	39.86	Urban	A1053	116.27	39.87
YG	116.15	39.82	Urban*	A1037	116.16	39.81
GC	116.18	39.91	Urban	A1019	116.21	39.92
FS	116.14	39.74	Rural	A1314	116.13	39.74
DX	116.40	39.72	Rural*	54594	116.35	39.72
YZ	116.51	39.80	Rural	54511	116.47	39.81
TZ	116.66	39.89	Rural	A1213	116.69	39.91
SY	116.66	40.13	Rural*	54398	116.62	40.13
CP	116.23	40.22	Rural*	54499	116.21	40.22
MTG	116.11	39.94	Rural*	A1354	116.11	39.94
PG	117.10	40.14	Rural*	54424	117.12	40.17
HR	116.63	40.33	Rural	A1621	116.63	40.32
MY	116.83	40.37	Rural*	54416	116.86	40.38
YQ	115.97	40.45	Rural	54406	115.97	40.45
QM	116.40	39.90	Traffic	A1001	116.39	39.90
YDM	116.39	39.88	Traffic	A1020	116.39	39.87
XZMB	116.35	39.95	Traffic	A1006	116.35	39.93
DL	116.22	40.29	Other*	A1407	116.25	40.29
BDL	115.99	40.37	Other	A1468	116.00	40.36
MYSK	116.91	40.50	Other*	A1655	116.85	40.47
DGC	117.12	40.10	Other*	A1514	117.14	40.08
YLD	116.78	39.71	Other	A1201	116.78	39.68
YF	116.30	39.52	Other	A1252	116.32	39.52

Note: The asterisk in the type column indicates that the underlying surface of the observing station is covered by
555 **vegetation.**

Table 2: Analysis of variance of each variable under different weather conditions (HWs, NHWs and precipitation).

	Source	SS	df	MS	F	P
Tmax	Group	2609.52	2	1304.76	215.27	1.09E-69
	Error	3315.38	547	6.06		
	Total	5924.89	549			
	Source	SS	df	MS	F	P
MDA8O$_3$	Group	204454.6	2	102227.3	56.32	6.03E-23
	Error	981941.2	541	1815		
	Total	1186396	543			
	Source	SS	df	MS	F	P
ER$_{HW}$	Group	2614.65	2	1307.33	221.48	3.46E-71
	Error	3228.8	547	5.9		
	Total	5843.45	549			
	Source	SS	df	MS	F	P
ER$_{ozone}$	Group	353.62	2	176.808	56.4	5.63E-23
	Error	1695.85	541	3.135		
	Total	2049.47	543			
	Source	SS	df	MS	F	P
ER$_{total}$	Group	4867.9	2	2433.94	207.28	1.69E-67
	Error	6329.2	539	11.74		
	Total	11197.1	541			

560   **Table 3: RH, temperature, HI, MDA8 O₃, O₃ concentration, and ER of HW and O₃ pollution compound events for mortalities in different station types associated with different weather conditions.**

Station type	Period	RH (%)	T_{mean} (°C)	T_{min} (°C)	T_{max} (°C)	HI_{mean} (°C)	HI_{min} (°C)	HI_{max} (°C)	MDA8 O₃ ($\mu g\ m^{-3}$)	O₃ mean ($\mu g\ m^{-3}$)	ER_{HW} (%)	ER_{Ozone} (%)	ER_{total} (%)
Urban	HWs	53.8	30.1	24.0	36.1	32.0	25.3	38.3	197.1	119.8	4.76(4.76,4.77)	8.01(0.79,16.00)	12.78(5.56,20.78)
	NHWs	62.4	26.6	21.6	31.8	27.8	22.0	33.3	158.5	91.5	0.3179(0.3175,0.3186)	6.40(0.64,12.70)	6.69(0.94,12.99)
	Precip	80.1	24.4	21.4	28.5	25.1	19.8	31.0	130.6	73.5	-2.868 (-2.866,-2.87)	5.24(0.52,10.36)	2.38(-2.34,7.49)
Rural	HWs	56.7	29.0	23.0	34.8	30.8	24.0	36.8	201.8	126.5	3.403(3.400,3.410)	8.21(0.81,16.42)	11.61(4.22,19.83)
	NHWs	64.5	25.7	20.7	30.7	26.9	21.3	32.0	161.0	96.6	-0.798(-0.797,-0.799)	6.50(0.65,12.92)	5.67(-0.17,12.08)
	Precip	79.1	23.9	20.8	27.8	24.7	19.7	30.0	135.7	79.4	-3.553(-3.550,-3.561)	5.45(0.54,10.79)	1.88(-3.02,7.21)
Traffic	HWs	50.3	30.4	25.2	35.8	32.1	26.7	37.6	169.7	118.9	4.412(4.408,4.421)	6.86(0.68,13.63)	11.28(5.09,18.06)
	NHWs	59.0	26.9	22.4	31.6	28.2	23.3	32.9	132.8	93.8	0.1092(0.1090,0.1095)	5.33(0.53,10.53)	5.42(0.63,10.61)
	Precip	77.3	24.5	21.6	28.5	25.3	20.3	30.6	106.2	78.7	-2.947(-2.944,-2.952)	4.24(0.43,8.35)	1.28(-2.54,5.38)
All	HWs	55.5	29.4	23.5	35.2	31.2	24.6	37.4	189.4	117.4	3.867(3.863,3.875)	7.90(0.78,15.78)	11.78(4.66,19.66)
	NHWs	63.8	25.9	21.1	31.0	27.2	21.6	32.6	151.4	89.6	-0.4179(-0.4175,-0.4187)	6.29(0.63,12.49)	5.85(0.2,12.03)
	Precip	79.7	24.0	20.9	28.0	24.7	19.7	30.4	125.9	72.5	-3.377(-3.374,-3.384)	5.23(0.52,10.33)	1.84(-2.86,6.94)
Ur–Ru	HWs	-2.9	1.0	1.1	1.3	1.2	1.3	1.5	-4.7	-6.7	1.36	-0.20	1.17
	NHWs	-2.2	0.9	0.9	1.1	0.9	0.7	1.3	-2.5	-5.1	1.12	-0.10	1.02
	Precip	0.9	0.5	0.5	0.7	0.4	0.1	1.0	-5.1	-5.9	0.08	-0.21	0.50

Note: Ur–Ru: Urban–Rural.

Table 4: RH, temperature, HI, MDA8 O$_3$, O$_3$ concentration, and ER of HW and O$_3$ compound pollution events for mortalities at different station types associated with different synoptic patterns.

Station type	Period	RH (%)	T_{mean} (°C)	T_{min} (°C)	T_{max} (°C)	HI_{mean} (°C)	HI_{min} (°C)	HI_{max} (°C)	MDA8 O$_3$ ($\mu g\ m^{-3}$)	O$_3$ mean ($\mu g\ m^{-3}$)	ER$_{HW}$ (%)	ER$_{Ozone}$ (%)	ER$_{compound}$ (%)
Urban	Type 1	55.9	30.3	24.6	36.0	32.8	26.0	39.2	216.3	133.1	4.65(4.64,4.66)	8.81(0.87,17.66)	13.45(5.50,22.30)
	Type 2	64.0	30.5	25.5	35.7	34.5	27.7	40.8	206.2	121.6	4.40(4.39,4.41)	8.38(0.83,16.76)	12.78(5.22,21.16)
	Type 3	49.7	29.5	22.6	36.4	29.9	23.2	36.4	201.4	122.4	5.06(5.05,5.07)	8.18(0.81,16.34)	13.24(5.86,21.41)
Rural	Type 1	58.2	29.4	23.6	34.8	31.6	24.8	37.7	225.6	142.6	3.381(3.378,3.388)	9.21(0.91,18.49)	12.59(4.28,21.88)
	Type 2	66.7	29.5	24.2	34.7	33.0	25.4	39.4	202.8	123.3	3.278(3.275,3.285)	8.24(0.81,16.46)	11.53(4.09,19.77)
	Type 3	53.0	28.4	21.5	35.0	28.9	22.0	35.0	201.3	127.4	3.538(3.534,3.545)	8.18(0.81,16.35)	11.71(4.33,19.89)
Traffic	Type 1	52.2	30.8	25.8	35.7	32.9	27.5	38.4	185.9	116.3	4.341(4.337,4.350)	7.53(0.75,15.02)	11.87(5.08,19.35)
	Type 2	59.7	30.8	26.5	35.6	34.4	29.3	39.5	175.8	101.2	4.161(4.157,4.170)	7.11(0.71,14.13)	11.24(4.83,18.27)
	Type 3	46.6	29.7	23.5	35.8	30.1	24.6	35.7	174.8	108.6	4.462(4.457,4.471)	7.06(0.70,14.03)	11.52(5.16,18.5)
All	Type 1	57.2	29.7	24.1	35.2	32.0	25.4	38.3	209.3	131.3	3.796(3.792,3.804)	8.80(0.87,17.63)	12.59(4.66,21.42)
	Type 2	65.5	29.8	24.7	35.0	33.5	26.5	39.9	195.0	114.5	3.644(3.640,3.651)	8.00(0.79,15.97)	11.66(4.44,19.64)
	Type 3	51.6	28.7	22.0	35.4	29.2	22.5	35.5	192.5	120.0	4.063(4.059,4.071)	7.99(0.79,15.95)	12.05(4.85,20.02)
Ur–Ru	Type 1	−2.37	1.0	1.0	1.2	1.1	1.1	1.5	-9.3	-9.5	1.27	−0.40	0.86
	Type 2	−2.74	1.0	1.3	1.0	1.4	2.3	1.4	3.4	-1.7	1.12	0.16	1.25
	Type 3	−3.31	1.1	1.1	1.4	1.1	1.2	1.4	0.1	-5.0	1.52	0	1.53

Table 5: Contribution rate of urbanization and weather type to ER.

Source	CR		
	ER_{HW}	ER_{ozone}	ER_{total}
urbanization	27.72%	-2.58%	8.08%
Type 1	85.36%	25.88%	46.39%
Type 2	84.51%	22.07%	43.58%
Type 3	86.54%	20.14%	45.54%

570